


SCIENTIFIC REPORTS



OPEN

Single injection of sustained-release prostacyclin analog ONO-1301-MS ameliorates hypoxic toxicity in the murine model of amyotrophic lateral sclerosis

Satoru Tada^{1,2}, Tatsusada Okuno¹, Mikito Shimizu¹, Yoshiki Sakai³, Hisae Sumi-Akamaru¹, Makoto Kinoshita¹, Kazuya Yamashita¹, Eri Sanda¹, Chi-Jing Choong¹, Akiko Namba¹, Tsutomu Sasaki¹, Toru Koda¹, Kazushiro Takata¹, Shigeru Miyagawa³, Yoshiki Sawa³, Yuji Nakatsuji¹ & Hideki Mochizuki¹ 

Amyotrophic lateral sclerosis (ALS) is a progressive neurodegenerative disease characterized by several pathologies including oxidative stress, apoptosis, neuroinflammation, and glutamate toxicity. Although multiple reports suggest that ischemia and hypoxia in the spinal cord plays a pivotal role in the pathogenesis of ALS, the precise role of hypoxia in disease progression remains unknown. In this study, we detected higher expression levels of Hypoxia-inducible factor 1-alpha (HIF-1 α), a key regulator of cellular responses to hypoxia, in the spinal cord of ALS patients and in the transgenic mice overexpressing the familial ALS-associated G93A SOD1 mutation (mSOD1^{G93A} mice) compared to controls. Single subcutaneous administration of sustained-release prostacyclin analog ONO-1301-MS to mSOD1^{G93A} mice abrogated the expression of HIF-1 α in their spinal cords, as well as erythropoietin (EPO) and vascular endothelial growth factor (VEGF), both of which are downstream to HIF-1 α . Furthermore, ONO-1301-MS increased the level of mature brain-derived neurotrophic factor (BDNF) and ATP production in the spinal cords of mSOD1^{G93A} mice. At late disease stages, the motor function and the survival of motor neurons of ONO-1301-MS-treated mSOD1^{G93A} mice was significantly improved compared to vehicle-treated mSOD1^{G93A} mice. Our data suggest that vasodilator therapy modulating local blood flow in the spinal cord has beneficial effects against ALS disease progression.

Amyotrophic lateral sclerosis (ALS) is a devastating disease characterized by progressive degeneration of motor neurons in the brain and spinal cord, resulting in muscle weakness. Although the precise mechanism of ALS remains unknown, it has become increasingly clear that ischemia and hypoxia are intimately involved in the pathogenesis of ALS¹⁻³. In fact, Hypoxia-inducible factor 1-alpha (HIF-1 α), a key regulator of cellular response to hypoxia, was highly expressed in the spinal cord of autopsy samples from ALS patients⁴. In addition, HIF-1 α has been shown to play a critical role in the pathogenesis of animal models of ALS^{4,5}.

Hypoxia is a risk factor for neurodegenerative diseases including Alzheimer's disease⁶, and it is a stress which is closely related to the clinical course of ALS; defects in hypoxic signaling have been reported in ALS patients and mSOD1^{G93A} mice⁷⁻¹⁰. Respiratory status is one of the prognostic factors for ALS patients, and respiratory impairment is an early sign of disease onset in mSOD1^{G93A} mice^{11,12}. Additionally, it has been becoming more and more clear that vascular changes are deeply involved in the pathogenesis of ALS¹³⁻¹⁶. Importantly, the blood-spinal cord

¹Department of Neurology, Osaka University Graduate School of Medicine, 2-2, Yamadaoka, Suita, Osaka, 565-0871, Japan. ²Department of Neurology, Tanaka Naika Medical Clinic, 2-7-28, Matsunohama-cho, Izumiotsu, Osaka, 595-0072, Japan. ³Department of Cardiovascular Surgery, Osaka University Graduate School of Medicine, 2-2, Yamadaoka, Suita, Osaka, 565-0871, Japan. Satoru Tada and Tatsusada Okuno and Mikito Shimizu contributed equally. Correspondence and requests for materials should be addressed to T.O. (email: okuno@neuro.med.osaka-u.ac.jp)

barrier (BSCB), which is composed of blood vessels and central nervous system (CNS), is damaged in human ALS patients and mSOD1^{G93A} mice, and the findings in mice show that BSCB breakdown plays a role in early-stage disease pathogenesis. In fact, reduced microcirculation in the spinal cord of mSOD1^{G93A} mice at both early¹³ and late¹⁶ disease stage are reported. However, whether anti-hypoxia therapy, which increases the blood flow and oxygen supply to the motor neurons in the spinal cord, has a positive impact on neurodegeneration in ALS remains elusive.

ONO-1301 is a synthetic prostacyclin agonist that includes a five-membered ring and allylic alcohol but lacks typical prostanoid structures¹⁷. It has thromboxane-synthase inhibitory activity, leading to stronger and longer-lasting blood vessel dilatation *in vivo* than other endothelin receptor antagonists or phosphodiesterase-5 inhibitors. Previous studies have shown that ONO-1301 treatment, by decreasing vascular tone and increasing blood flow, ameliorates not only monocrotaline-induced pulmonary hypertension but also neurological dysfunction in rats with cerebral infarction^{17,18}. More recently, a novel sustained-release ONO-1301 (ONO-1301-MS) has been developed by polymerizing ONO-1301 with poly (D,L-lactic-co-glycolic acid) (PLGA) microspheres¹⁹. A single subcutaneous injection of ONO-1301-MS resulted in sustained elevation of ONO-1301 levels for 12 weeks²⁰.

In this study, we confirmed enhanced immunoreactivity of HIF-1 α in the spinal cord of ALS patients and in transgenic mice overexpressing the familial ALS-associated G93A SOD1 mutation (mSOD1^{G93A} mice). To investigate the potential efficacy of anti-hypoxia therapy in ALS, we assessed the effect of ONO-1301-MS, a sustained-release form of ONO-1301, on disease progression in mSOD1^{G93A} mice.

Results

Elevated expression of HIF-1 α suggests hypoxia in the spinal cords of ALS patients and transgenic ALS mice.

We investigated HIF-1 α expression as a marker for hypoxia and ischemia in autopsied spinal cord specimens from ALS patients and spinal cord samples of mSOD1^{G93A} mice. Increased HIF-1 α immunoreactivity was detected in the anterior horn cells from ALS cases compared to controls (Supplementary Fig. S1a,b). Quantitative analysis showed that HIF-1 α expression was significantly higher in the ALS group than in the control group (Supplementary Fig. S1c, $P < 0.05$, Mann-Whitney U test). Similar findings were detected in mSOD1^{G93A} mice compared to age-matched, wild-type mice (Supplementary Fig. S1d-f). These data are consistent with previous reports of hypoxia in the spinal cords of ALS patients¹ and in the ALS mice model⁴.

ONO-1301 protects against neurodegeneration in the mSOD1^{G93A} mouse model of ALS by suppressing hypoxic stress.

To explore the therapeutic effect of increased blood flow in ALS, we subcutaneously administered ONO-1301-MS, a sustained-release form of ONO-1301, or vehicle (PLGA) to mSOD1^{G93A} mice on day 64 of age. We were able to detect measurable concentrations of ONO-1301 in serum of ONO-1301-MS-treated mSOD1^{G93A} mice (Fig. 1a). Next, we measured the motor performance of both groups using the rotarod machine. ONO-1301-MS administration significantly improved the motor function of mSOD1^{G93A} mice at 17 weeks of age ($P = 0.035$, Mann-Whitney U test) and 20 weeks of age ($P = 0.025$, Mann-Whitney U test) (Supplementary Fig. S2a). Moreover, we found that ONO-1301-MS-treated mSOD1^{G93A} mice had increased body weight compared to control mice (Supplementary Fig. S2b, $P < 0.01$, repeated measures ANOVA for week 17 to week 20). Consistent with these observations, Nissl staining revealed that treatment with ONO-1301-MS resulted in increased motor neuron survival in the spinal cords of mSOD1^{G93A} mice at 17 weeks of age (Figs 1b and S2c). ONO-1301 had no significant impact on average survival time (Supplementary Fig. S2d, $P = 0.99$, log-rank test) and microglial/astroglial activation (Fig. 1c-h) in mSOD1^{G93A} mice. Collectively, these results suggest that ONO-1301 treatment improved motor function and ameliorated neurodegeneration of mSOD1^{G93A} mice at late stage of disease by suppressing hypoxic stress, though it did not affect neuroinflammation.

ONO-1301 mitigated hypoxia in the spinal cord of mSOD1^{G93A} mice.

In order to confirm that the favorable effects by ONO-1301 were mediated through its anti-hypoxic activity, we examined the expression level of HIF-1 α in the spinal cords of ONO-1301-MS-treated mSOD1^{G93A} mice and vehicle-treated controls. Western blot analysis of spinal cord extracts revealed significantly lower expression of HIF-1 α following ONO-1301 treatment, suggesting that it alleviated hypoxia in the spinal cord of mSOD1^{G93A} mice (Fig. 2a). Next, we performed immunohistochemical staining to determine the localization of HIF-1 α in the spinal cord of mSOD1^{G93A} mice. We observed the significantly decreased immunoreactivity against HIF-1 α in the spinal cord of ONO-1301-MS-treated mSOD1^{G93A} mice (Fig. 2b). HIF-1 α was largely localized in the cytoplasm of neuron-like cells. In addition, qPCR analysis demonstrated that ONO-1301 abrogated the transcription of erythropoietin (EPO) and vascular endothelial growth factor (VEGF), both of which are downstream molecules to HIF-1 α , in the spinal cord of mSOD1^{G93A} mice (Fig. 2c), but not osteopontin (OPN), which is another marker of hypoxia²¹ (Fig. 2d). Collectively, these data suggest that ONO-1301 successfully ameliorated hypoxia in the spinal cord of mSOD1^{G93A} mice and alleviated neurodegeneration in this animal model of ALS.

ONO-1301 increases ATP production, suggesting that it alleviates hypoxia in the spinal cord of mSOD1^{G93A} mice.

Following cerebral ischemia, various molecules related to inflammation, apoptosis, trophic factors, and transcription factors are induced, and some of these molecules are known to be involved in neurodegeneration of ALS. To clarify the mechanisms of actions related to the efficacy of ONO-1301, we compared the expression levels of molecules associated with these pathways in the spinal cord of ONO-1301-MS-treated and vehicle-treated mSOD1^{G93A} mice using semi-quantitative RT-PCR. ONO-1301 had no significant effects on the expression levels of molecules related to inflammation, trophic factors, and transcription factors involving ischemia such as cAMP response element binding protein (Creb) and proliferator-activated receptor gamma coactivator 1-alpha (PGC1a) (Fig. 3a). Importantly, ONO-1301 administration significantly

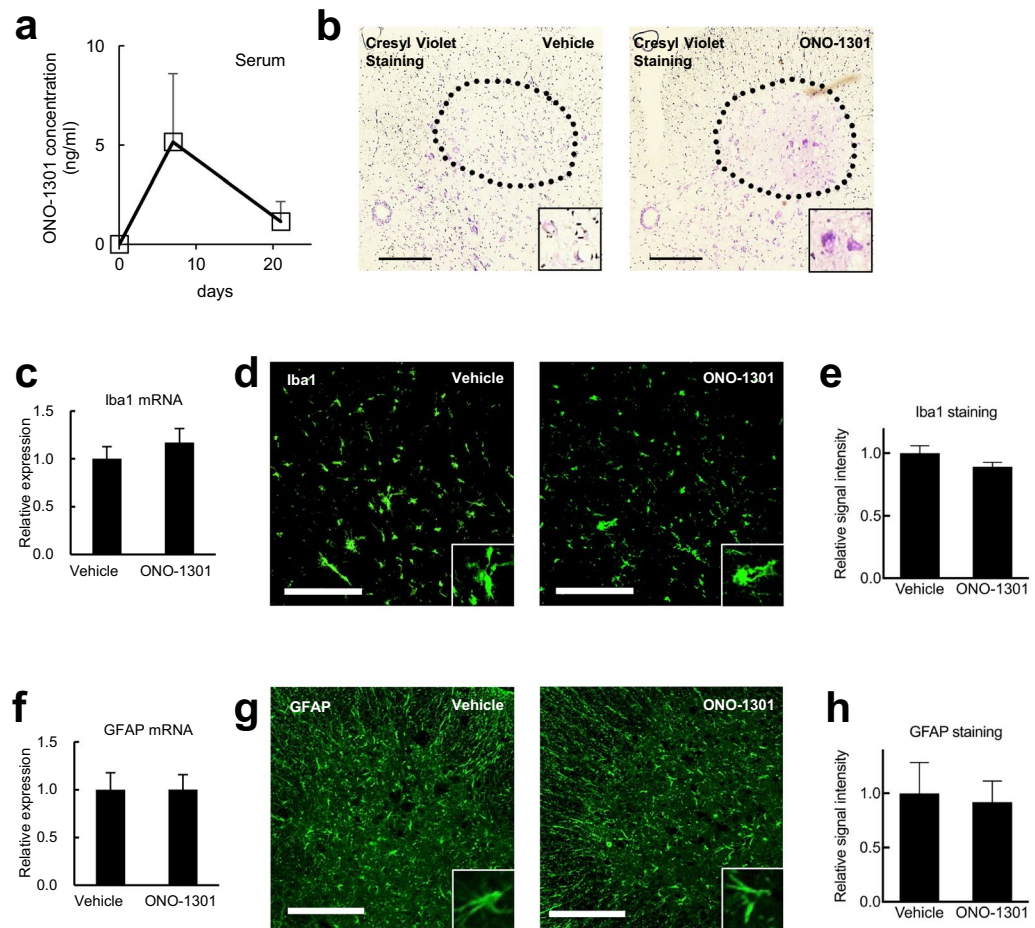


Figure 1. ONO-1301 preserved motor neurons in $mSOD1^{G93A}$ mouse model of ALS without affecting neuroinflammation. **(a)** Serum concentrations of ONO-1301 after subcutaneous administration of ONO-1301-MS were evaluated. Effective blood concentrations were maintained after 21 days of administration (serum ONO-1301 concentration, 5.15 ± 3.45 ng/ml (7 days), 1.15 ± 1.02 ng/ml (21 days), mean \pm SEM). **(b)** Histological analysis revealed that ONO-1301-MS administration preserved the number of motor neurons in the ventral horn of the lumbar spinal cords of $mSOD1^{G93A}$ mice at 120 days of age. Representative images of sections that were stained with cresyl violet are shown. **(c–h)** Microgliosis and astrogliosis in the spinal cords of ONO-1301-MS-treated $mSOD1^{G93A}$ mice and vehicle-treated control mice. Quantitative RT-PCR analyses for the expression of Iba1 **(c)** and GFAP **(f)** mRNAs in whole spinal cord samples ($n = 5$ mice per condition) from ONO-1301-MS-treated $mSOD1^{G93A}$ mice and vehicle-treated control mice at 120 days of age. Sections of the lumbar cord were stained with an anti-Iba1 **(d)** or with an anti-GFAP antibody **(g)**, and relative fluorescence signal intensities were quantified by ImageJ **(e,h)**. Scale bar = 200 μ m. Data are expressed as the mean \pm SEM. * $P < 0.05$, ** $P < 0.01$.

increased the level of mature BDNF in the spinal cord of $mSOD1^{G93A}$ mice (Fig. 3b). Although ONO-1301 significantly decreased the expression level of caspase-9 (Casp9), a key molecule in the mitochondrial apoptosis pathway (Fig. 3c), western blot analysis did not reveal any significant effects on the cleavage of active caspase-9 (data not shown). Similarly, ONO-1301 had no obvious effect on the transcriptional levels of other molecules that are involved in apoptosis (Fig. 3d).

Given that ischemia and hypoxia usually cause deprivation of mitochondrial ATP production, we sought to determine whether ONO-1301 treatment increased ATP concentration in the spinal cord of $mSOD1^{G93A}$ mice. We confirmed that ONO-1301-MS treatment significantly restored ATP concentration, suggesting increased ATP production from the mitochondria and improved blood supply in the spinal cord of $mSOD1^{G93A}$ mice (Fig. 3e). Taken together, these data suggest that ONO-1301 alleviated hypoxia in the spinal cords and prevented neurodegeneration in $mSOD1^{G93A}$ mice partly through increasing BDNF and restoring mitochondrial functions.

Discussion

In this study, we showed that treatment with a prostacyclin agonist successfully ameliorated the motor functions of $mSOD1^{G93A}$ mice and prevented their body weight loss. The beneficial effects of prostacyclin agonist treatment in ALS mice were partly mediated by alleviating hypoxia and hypo-perfusion in the spinal cord, leading to the increased ATP production. Moreover, we have shown that increasing blood flow in hypoxic regions of the spinal

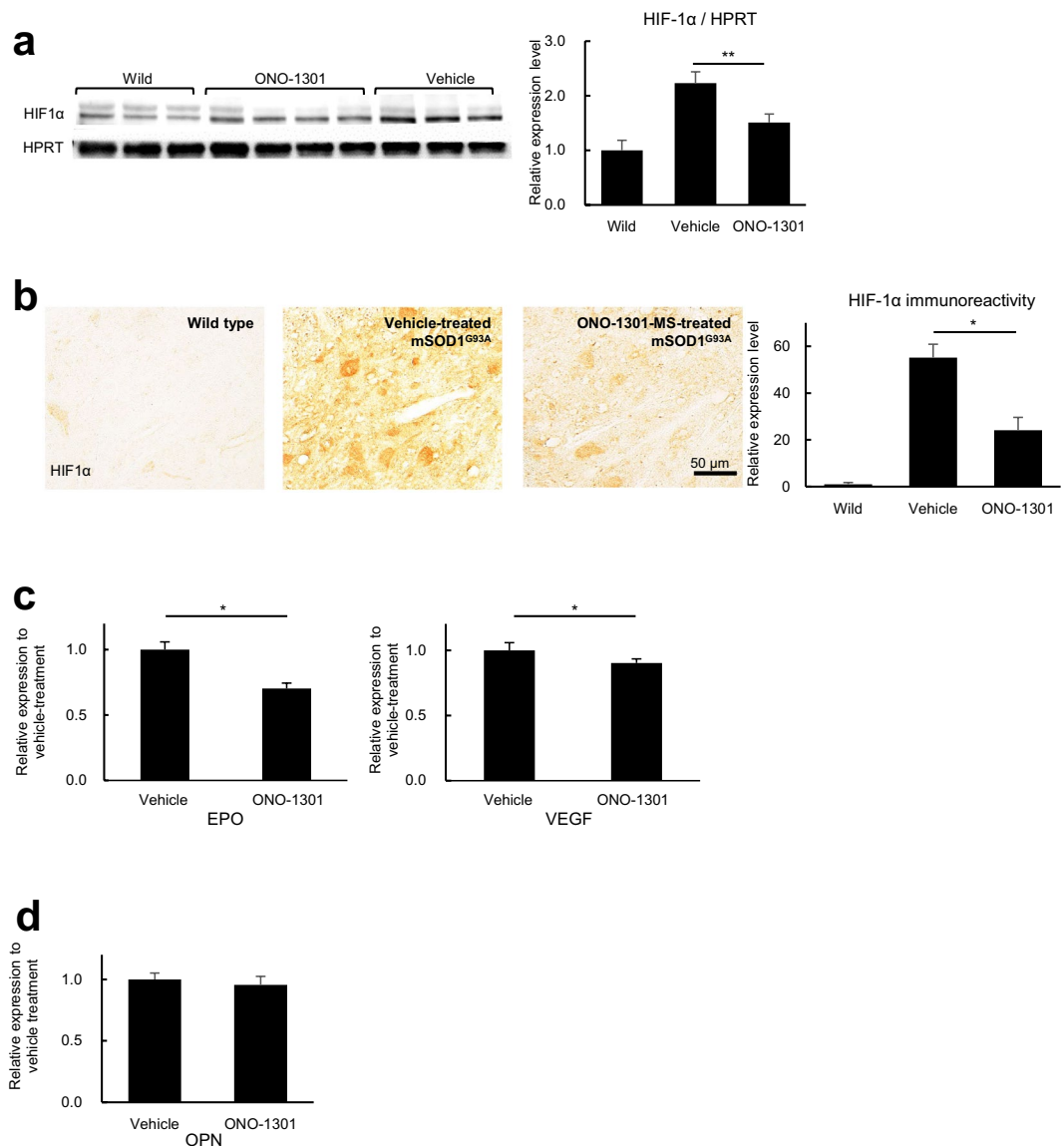


Figure 2. ONO-1301 ameliorates hypoxia in the spinal cord of $mSOD1^{G93A}$ mice. **(a)** Western blot analysis revealed significantly decreased HIF-1 α expression in the spinal cords of 120-day-old ONO-1301-MS-treated $mSOD1^{G93A}$ mice relative to vehicle-treated $mSOD1^{G93A}$ mice. **(b)** Fixed frozen sections of lumbar cord of $mSOD1^{G93A}$ mice were stained with anti-HIF-1 α antibodies. Representative images show reduced immunoreactivity of HIF-1 α in 120-day-old ONO-1301-MS-treated $mSOD1^{G93A}$ mice compared to age-matched vehicle-treated control mice ($n = 3$ mice per group). Scale bar = 50 μ m. **(c,d)** Quantitative RT-PCR analyses for erythropoietin (EPO), vascular endothelial growth factor (VEGF) (c) and osteopontin (OPN) (d) in spinal cords of ONO-1301-MS-treated $mSOD1^{G93A}$ mice and vehicle-treated control mice at 120 days of age ($n = 5$ per group). The expression levels of EPO ($P = 0.014$) and VEGF ($P = 0.036$) were significantly reduced in the ONO-1301-MS-treated group. Data are expressed as the mean \pm SEM. * $P < 0.05$, ** $P < 0.01$.

cord might play an important role in protecting against neurodegeneration in an animal model of ALS. To the best of our knowledge, this is the first report that suggests anti-hypoxia treatment could be a therapeutic option for the treatment of ALS.

We showed that HIF-1 α expression was decreased in the spinal cord of ONO-1301-MS-treated $mSOD1^{G93A}$ mice. This was accompanied by lower transcription levels of EPO and VEGF, which have been reported to be neuroprotective in the pathogenesis of ALS²². Anti-hypoxia therapy using ONO-1301, which improved mitochondrial energy production, could counteract the negative effects of downregulating neuroprotective factors including VEGF. In fact, decrease in transcriptional level of VEGF by ONO-1301 was subtle.

An increasing number of researchers have revealed that hypoxia and ischemia are intimately involved in the pathogenesis of ALS¹⁶. Recently, Sun *et al.* reported that repeated transient ischemia upregulates TAR DNA-binding protein 43 (TDP-43), which is a key molecule in the pathogenesis of ALS²³. Another group reported that overexpression of TDP-43 is toxic to motor neurons²⁴. Collectively, these reports suggest that anti-hypoxia

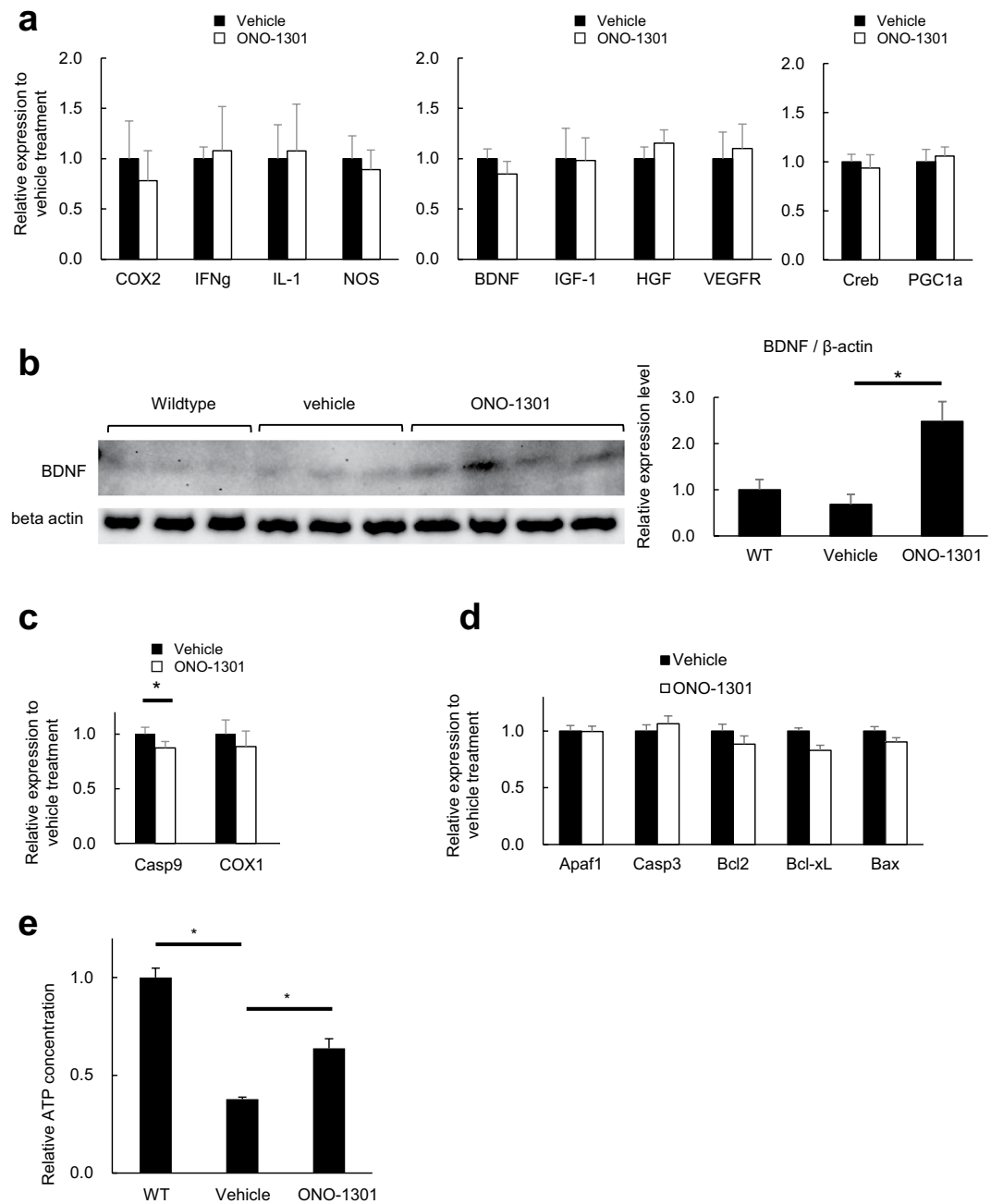


Figure 3. ONO-1301 increased mature BDNF and ATP production in the spinal cord of $mSOD1^{G93A}$ mice. **(a)** Relative mRNA expression levels of cyclooxygenase 2 (COX2), interferon gamma (IFN-g), interleukin 1 beta (IL-1), nitric oxide synthase 2 (NOS), brain-derived neurotrophic factor (BDNF), insulin-like growth factor 1 (IGF-1), hepatocyte growth factor (HGF), vascular endothelial growth factor receptor (VEGFR), cAMP response element binding protein (Creb), and peroxisome proliferator-activated receptor gamma coactivator 1-alpha (PGC1a) in the spinal cord of 120-day-old ONO-1301-MS-treated $mSOD1^{G93A}$ mice and vehicle-treated controls. **(b)** Western blot analysis revealed significantly increased level of mature BDNF in the spinal cords of 120-day-old ONO-1301-MS-treated $mSOD1^{G93A}$ mice relative to vehicle-treated $mSOD1^{G93A}$ mice. **(c)** Relative mRNA expression levels of caspase-9 (Casp9) and cyclooxygenase 1 (COX1) in the spinal cord of 120-day-old ONO-1301-MS-treated $mSOD1^{G93A}$ mice and vehicle-treated controls. **(d)** Relative mRNA expression levels of Apoptotic protease activating factor 1 (Apaf1), caspase 3 (Casp3), B-cell lymphoma 2 (Bcl2), B-cell lymphoma-extra large (Bcl-xL), and BCL2 associated X (Bax) in the spinal cord of 120-day-old ONO-1301-MS-treated $mSOD1^{G93A}$ mice and vehicle-treated controls. **(e)** ATP concentrations in spinal cords of ONO-1301-MS-treated $mSOD1^{G93A}$ mice and vehicle-treated $mSOD1^{G93A}$ mice at 12 weeks of age ($n = 3$ mice per group) after 3 weeks of treatment. The values were normalized to basal levels in wild-type mice or in vehicle-treated $mSOD1^{G93A}$ mice. Data are expressed as the mean \pm SEM. $*P < 0.05$.

therapy using ONO-1301 could ameliorate the motor symptom of ALS by reducing the expression levels of TDP-43. In addition, overexpression of mutant SOD1^{G93A} in human neuronal cells decreased cell viability and disabled autophagy when cultured in a low O₂ environment⁹. Given that motor neurons in patients with ALS have a higher susceptibility to hypoxic stress, anti-hypoxia treatment could be a useful target for the treatment of ALS.

Regarding the mechanisms by which ONO-1301 had a positive impact on neurodegeneration in animal models of ALS, we consider that not only its anti-hypoxia effect but also its effect against pericytes is important. In fact, several reports suggest that pericytes are deeply involved not only in the physiological activity of brain but also in the pathogenesis of neurodegenerative diseases such as ALS^{25–29}. Notably, pericytes extend the survival of ALS mice²⁷, suggesting that increasing the number of pericytes could be a therapeutic option in the treatment of ALS. Importantly, prostacyclin recruits pericytes³⁰ and suppress the loss of pericytes in central nervous system³¹. Collectively, these results raise the possibility that ONO-1301 suppressed neurodegeneration in mSOD1^{G93A} mice partly through acting on pericytes.

ONO-1301-MS treatment successfully prevented the loss of motor neurons in the spinal cord of mSOD1^{G93A} mice at end-stage but failed to prolong their overall survival. This may be partly due to the inability of ONO-1301 to fully alleviate the hypoxic stress induced in mSOD1^{G93A} mice. Indeed, ONO-1301 did not demonstrate significant suppression of pro-inflammatory (Fig. 3a) nor pro-apoptotic molecules (Fig. 3d), which are strongly implicated in the pathogenesis of ALS^{32–36}. More potent anti-hypoxic therapies or combination therapies targeting cascades other than hypoxia may be required to prolong overall survival.

We showed that ONO-1301-MS treatment increased the blood flow and suppressed hypoxia in the spinal cord of mSOD1^{G93A} mice. On the other hand, it might have increased the leakage of neurotoxins by increasing blood flow in compromised microcapillaries in the spinal cord of mSOD1^{G93A} mice, leading to the minimal neuroprotective effect. In fact, recent reports by Winkler *et al.* and Zhong *et al.* suggest that blood-spinal-cord barrier (BSCB) in mSOD1^{G93A} mice is compromised at early-stage of the disease, and activated protein C (APC) and its analog restored the disrupted BSCB in mSOD1^{G93A} mice and contributed to protecting from motor neuronal degeneration^{14,15,28}. Based on their results and ours, combination therapy with ONO-1301-MS and APC could be a more promising option for the treatment of ALS by increasing blood flow in repaired microcapillaries in the spinal cord.

Although additional studies are needed to clarify the potential role of hypoxia in ALS, our findings highlight the therapeutic potential of targeting the hypoxia/hypo-perfusion axis for the treatment of ALS. Thus, a treatment modality that inhibits hypoxia holds great therapeutic promise for treating ALS patients.

Methods

Tissue sources of autopsied spinal cord. The research presented in this study was approved by the Ethics Committee of Osaka University Graduate School of Medicine (permit number 10038, 25-079-005, Biken-AP-H21-28-0). Lumbar cord specimens were obtained at autopsy from ALS patients and other neurological disease control patients (one multiple system atrophy (MSA) and two familial amyloid polyneuropathy (FAP) patients). Consent for autopsy was obtained from legal representatives for all subjects in accordance with the local institutional review board requirements, which were approved by the Ethics Committee of Osaka University Graduate School of Medicine. All neuropathologic analyses were performed by trained neuropathologists.

Preparation of ONO-1301-MS. ONO-1301 was synthesized by ONO Pharmaceutical, (Osaka, Japan) as previously described^{137–139}. A sustained-release form of ONO-1301 (ONO-1301-MS) was generated by encapsulating ONO-1301 with poly (D,L-lactic-co-glycolic acid) (PLGA) as described previously^{19,40}. Briefly, polyvinyl alcohol aqueous solution (poor solvent of PLGA) was put into a glass vessel. An ethanol/dichloromethane solution containing PLGA and ONO-1301 was dropped into the poor solvent while stirring to form an oil-in-water emulsion. Dichloromethane was then evaporated off by stirring at room temperature. After centrifugation and washing, ONO-1301-PLGA microspheres were isolated by lyophilization.

Animals and treatment with ONO-1301-MS. mSOD1^{G93A} mice were obtained from The Jackson Laboratory (strain designated: B6SJL-TgN(SOD1-G93A)1Gurd/J) and backcrossed with C57BL/6 mice for at least ten generations. ONO-1301-MS (250 mg/kg) was administered via subcutaneous injections into the backs of mice as previously described³⁹. For the measurement of ATP, ONO-1301-MS was administered to 9-week-old mSOD1^{G93A} mice and they were sacrificed after 3 weeks of administration. For the other experiments, ONO-1301-MS was administered at 64 days of age.

Assay of serum level of ONO-1301. The whole blood was taken from mice and allowed to clot by leaving it undisturbed at room temperature for 30 minutes. The clot was removed by centrifugation at 1000g for 10 min in a refrigerated centrifuge. Serum ONO-1301 levels were measured by liquid chromatography with tandem mass spectrometric assay.

Motor neuron counts. mSOD1^{G93A} mice at 120 days were sacrificed and perfused with 4% paraformaldehyde in PBS, and lumbar spinal cords were dissected out. Spinal cords were dehydrated in increasing alcohol concentrations, before embedding in paraffin. For motor neuron counts, 20 serial horizontal sections of the L5 segment of spinal cord (10 μm thick) were cut using a microtome and mounted onto slides. Cresyl violet staining was performed on the 5th, 10th, 15th and 20th serial sections and motor neurons in both ventral horns on each section were counted within an area defined by a horizontal line through the central canal. Four male animals in ONO-1301-MS-treated group and 6 male animals in vehicle-treated group were analyzed. These experiments were conducted in a blinded fashion.

Immunohistochemistry. Fixed frozen sections of spinal cord from mSOD1^{G93A} mice (10 μm thick) were prepared as previously described³². Hypoxia-induced factor 1-alpha (HIF-1α) expression was evaluated in paraffin-embedded 6-μm-thick sections of the lumbar cord from ALS patients and 10 μm-thick fixed frozen sections of spinal cord of mSOD1^{G93A} mice as previously described⁴¹. The following primary antibodies were used: rabbit anti-HIF-1α polyclonal antibody (1:100; Novus Biologicals), rabbit anti-Iba1 polyclonal antibody (1:1000, Wako) and Alexa Fluor 488[®]-conjugated mouse anti-gial fibrillary acidic protein (GFAP) monoclonal antibody (1:200; Cell Signaling Technology). The following secondary antibodies were used: AlexaFlour488-conjugated goat anti-rabbit IgG antibody (1:500, Invitrogen) and goat anti-rabbit immunoglobulins conjugated to peroxidase-labeled dextran polymer (Dako Envision+, Dako). For HIF-1α staining, reaction products were visualized with 3,3'-diaminobenzidine tetrahydrochloride (Vector Laboratories). The relative optical densities of HIF-1α immunoreactivity were quantified using ImageJ. The fluorescently labeled sections were examined using an LSM 510 confocal microscope (Zeiss).

Western blotting. Western blot analysis was performed as previously described⁴². Samples were lysed with NP-40 buffer [PBS, 01% TritonX, 05% sodium deoxycholate, 01% sodium dodecyl sulfate (SDS), 50 mM Tris-HCl and 150 mM NaCl, pH 80] containing protease inhibitors (20 mg/ml aprotinin and 1 mM phenylmethylsulfonyl fluoride), 2-mercaptoethanol and 1 mM sodium orthovanadate. Equal concentrations of protein were resolved on 10% SDS-polyacrylamide gels, and then transferred onto Poly-vinylidene Difluoride (PVDF) membranes (ATTO, Tokyo, Japan). The blots were incubated at 4 °C overnight with one of the following primary antibodies: rabbit anti-HIF-1α polyclonal antibody (1:500; Novus Biologicals), rabbit anti-HPRT monoclonal antibody (1:2000; abcam), rabbit anti-BDNF monoclonal antibody (1:500; abcam), mouse anti-β-actin monoclonal antibody (1:10000; Sigma-Aldrich). The blots were subsequently incubated with the appropriate horseradish peroxidase-conjugated secondary antibodies for 90 min and visualized using SuperSignal West Femto Maximum Sensitivity Substrate (Thermo Fisher Scientific, Waltham, MA, USA). The image of each band was captured and analyzed using Image Gauge (Fuji Film, Japan) and ImageJ.

RNA extraction and RT-qPCR analysis. Total RNA and cDNA from spinal cords of ONO-1301-MS-treated mSOD1^{G93A} mice at 120 days of age and age-matched control mice were generated as previously described³⁵. cDNA was amplified using SYBR Premix Ex Taq II (Takara Bio) and analyzed as previously described³⁶.

Measurement of ATP. Spinal cord tissue was homogenized in sterilized ultrapure water on ice and the lysates were centrifuged at 1000 g for 5 min. Extractions of ATP were performed using an AMERIC-ATP kit (AMERIC, Japan), and the fluorescence in each sample was measured using Lumat3 (LB9508, BERTHOLD).

Statistical analysis. Student's *t*-test was used to compare two groups and an ANOVA was used to compare more than two groups. Data are expressed as the mean ± SEM. *P*-values less than or equal to 0.05 were considered statistically significant.

Ethics approval and consent to participate. The present study was conducted according to the revised Declaration of Helsinki and Good Clinical Practice guidelines and was approved by the local ethics committees. Informed consent was given by all study participants or their legal representative. All animal experiments were performed in compliance with the Japanese national guidelines and the guidelines of Osaka University, which specifically approved this study (Permit number: Biken-AP-H21-28-0).

Data Availability

The datasets used and/or analyzed during the current study are available from the corresponding author on reasonable request.

References

- Lambrechts, D. *et al.* VEGF is a modifier of amyotrophic lateral sclerosis in mice and humans and protects motoneurons against ischemic death. *Nat. Genet.* **34**, 383–394 (2003).
- Kim, S. H. S. M. *et al.* Intermittent hypoxia can aggravate motor neuronal loss and cognitive dysfunction in ALS mice. *PLoS One* **8**, 1–10 (2013).
- Turner, M. R., Goldacre, R., Talbot, K. & Goldacre, M. J. Cerebrovascular injury as a risk factor for amyotrophic lateral sclerosis. *J. Neurol Neurosurg Psychiatry* **87**, 244–246 (2015).
- Nagara, Y. *et al.* Impaired cytoplasmic-nuclear transport of hypoxia-inducible factor-1α in amyotrophic lateral sclerosis. *Brain Pathol.* **23**, 534–546 (2013).
- Sato, K. *et al.* Impaired response of hypoxic sensor protein HIF-1α and its downstream proteins in the spinal motor neurons of ALS model mice. *Brain Res.* **1473**, 55–62 (2012).
- Zhang, X. & Le, W. Pathological role of hypoxia in Alzheimer's disease. *Experimental Neurology* **223**, 299–303 (2010).
- Büchner, M. *et al.* Impaired tolerance to repetitive hypoxia in hippocampal slices of Cu,Zn superoxide dismutase transgenic mice. *Neurosci. Lett.* **276**, 131–134 (1999).
- Moreau, C. *et al.* Deregulation of the hypoxia inducible factor-1α pathway in monocytes from sporadic amyotrophic lateral sclerosis patients. *Neuroscience* **172**, 110–117 (2011).
- Xu, R. *et al.* Linking hypoxic and oxidative insults to cell death mechanisms in models of ALS. *Brain Res.* **1372**, 133–144 (2011).
- Zhang, Z., Yan, J., Chang, Y., ShiDu Yan, S. & Shi, H. Hypoxia Inducible Factor-1 as a Target for Neurodegenerative Diseases. *Curr. Med. Chem.* **18**, 4335–4343 (2011).
- Tankersley, C. G., Haenggeli, C. & Rothstein, J. D. Respiratory impairment in a mouse model of amyotrophic lateral sclerosis. *J. Appl. Physiol.* **102**, 926–32 (2007).
- Beghi, E. *et al.* The epidemiology and treatment of ALS: Focus on the heterogeneity of the disease and critical appraisal of therapeutic trials. *Amyotroph. Lateral Scler.* **12**, 1–10 (2011).
- Zhong, Z. *et al.* ALS-causing SOD1 mutants generate vascular changes prior to motor neuron degeneration. *Nat. Neurosci.* **11**, 420–422 (2008).

14. Winkler, E. A. *et al.* Blood-spinal cord barrier disruption contributes to early motor-neuron degeneration in ALS-model mice. *Proc. Natl. Acad. Sci.* **111**, E1035–E1042 (2014).
15. Zhong, Z. *et al.* Activated protein C therapy slows ALS-like disease in mice by transcriptionally inhibiting SOD1 in motor neurons and microglia cells. *J. Clin. Invest.* **119**, 3437–3449 (2009).
16. Miyazaki, K. *et al.* Early and Progressive Impairment of Spinal Blood Flow—Glucose Metabolism Coupling in Motor Neuron Degeneration of ALS Model Mice. *J. Cereb. Blood Flow Metab.* **32**, 456–467 (2012).
17. Kataoka, M. *et al.* A long-acting prostacyclin agonist with thromboxane inhibitory activity for pulmonary hypertension. *Am. J. Respir. Crit. Care Med.* **172**, 1575–1580 (2005).
18. Hazekawa, M., Sakai, Y., Yoshida, M., Haraguchi, T. & Uchida, T. Single injection of ONO-1301-loaded PLGA microspheres directly after ischaemia reduces ischaemic damage in rats subjected to middle cerebral artery occlusion. *J. Pharm. Pharmacol.* **64**, 353–359 (2012).
19. Obata, H. *et al.* Single injection of a sustained-release prostacyclin analog improves pulmonary hypertension in rats. *Am. J. Respir. Crit. Care Med.* **177**, 195–201 (2008).
20. Sawa, Y. *et al.* Advanced heart failure treatment material as myocardial/cardiovascular regeneration device. Available at, <http://patft.uspto.gov/netacgi/nph-Parser?Sect1=PTO2&Sect2=HITOFF&p=1&u=%2Fnetacgi%2FPTO%2Fsearch-adv.htm&r=1&f=G&l=50&d=PTXT&S1=9597436.PN.&OS=PN/9597436&RS=PN/9597436> (2017).
21. Sodhi, C. P., Phadke, S. A., Batlle, D. & Sahai, A. Hypoxia and high glucose cause exaggerated mesangial cell growth and collagen synthesis: role of osteopontin. *Am. J. Physiol. Renal Physiol.* **280**, F667–74 (2001).
22. Zheng, C., Nennesmo, I., Fadeel, B. & Henter, J.-I. Vascular endothelial growth factor prolongs survival in a transgenic mouse model of ALS. *Ann. Neurol.* **56**, 564–567 (2004).
23. Sun, M. *et al.* Acceleration of TDP43 and FUS/TLS protein expressions in the preconditioned hippocampus following repeated transient ischemia. *J. Neurosci. Res.* **92**, 54–63 (2014).
24. Ash, P. E. A. *et al.* Neurotoxic effects of TDP-43 overexpression in *C. elegans*. *Hum. Mol. Genet.* **19**, 3206–3218 (2010).
25. Nikolakopoulou, A. M., Zhao, Z., Montagne, A. & Zlokovic, B. V. Regional early and progressive loss of brain pericytes but not vascular smooth muscle cells in adult mice with disrupted platelet-derived growth factor receptor- β signaling. *PLoS One* **12**, 1–19 (2017).
26. Rustenhoven, J., Jansson, D., Smyth, L. C. & Dragunow, M. Brain Pericytes As Mediators of Neuroinflammation. *Trends Pharmacol. Sci.* **38**, 291–304 (2017).
27. Coatti, G. C. *et al.* Pericytes Extend Survival of ALS SOD1 Mice and Induce the Expression of Antioxidant Enzymes in the Murine Model and in iPSCs Derived Neuronal Cells from an ALS Patient. *Stem Cell Rev. Reports* **13**, 686–698 (2017).
28. Winkler, E. A. *et al.* Blood-spinal cord barrier breakdown and pericyte reductions in amyotrophic lateral sclerosis. *Acta Neuropathol.* **125**, 111–120 (2013).
29. Garbuzova-Davis, S. & Sanberg, P. R. Blood-CNS Barrier Impairment in ALS patients versus an animal model. *Front. Cell. Neurosci.* **8**, 1–9 (2014).
30. Minami, Y. *et al.* Prostaglandin I2 analog suppresses lung metastasis by recruiting pericytes in tumor angiogenesis. *Int. J. Oncol.* **46**, 548–554 (2015).
31. Muramatsu, R. *et al.* Prostacyclin prevents pericyte loss and demyelination induced by lysophosphatidylcholine in the central nervous system. *J. Biol. Chem.* **290**, 11515–11525 (2015).
32. Okuno, T. *et al.* Induction of cyclooxygenase-2 in reactive glial cells by the CD40 pathway: Relevance to amyotrophic lateral sclerosis. *J. Neurochem.* **91**, 404–412 (2004).
33. Barber, S. C. & Shaw, P. J. Oxidative stress in ALS: key role in motor neuron injury and therapeutic target. *Free Radic. Biol. Med.* **48**, 629–41 (2010).
34. Philips, T. & Robberecht, W. Neuroinflammation in amyotrophic lateral sclerosis: role of glial activation in motor neuron disease. *Lancet Neurol.* **10**, 253–63 (2011).
35. Tada, S. *et al.* Deleterious effects of lymphocytes at the early stage of neurodegeneration in an animal model of amyotrophic lateral sclerosis. *J. Neuroinflammation* **8**, 19 (2011).
36. Tada, S. *et al.* Partial suppression of M1 microglia by Janus kinase 2 inhibitor does not protect against neurodegeneration in animal models of amyotrophic lateral sclerosis. *J. Neuroinflammation* **11**, 179 (2014).
37. Hayashi, K., Nagamatsu, T., Oka, T. & Suzuki, Y. Modulation of anti-glomerular basement membrane nephritis in rats by ONO-1301, a non-prostanoid prostaglandin I2 mimetic compound with inhibitory activity against thromboxane A2 synthase. *Jpn J Pharmacol* **73**, 73–82 (1997).
38. Imawaka, H. & Sugiyama, Y. Kinetic study of the hepatobiliary transport of a new prostaglandin receptor agonist. *J. Pharmacol. Exp. Ther.* **284**, 949–57 (1998).
39. Murakami, S. Prostacyclin agonist with thromboxane synthase inhibitory activity (ONO-1301) attenuates bleomycin-induced pulmonary fibrosis in mice. *AJP Lung Cell. Mol. Physiol.* **290**, L59–L65 (2005).
40. Iwata, H. *et al.* Local delivery of synthetic prostacycline agonist augments collateral growth and improves cardiac function in a swine chronic cardiac ischemia model. *Life Sci.* **85**, 255–261 (2009).
41. Sumi, H. *et al.* Nuclear TAR DNA binding protein 43 expression in spinal cord neurons correlates with the clinical course in amyotrophic lateral sclerosis. *J. Neuropathol. Exp. Neurol.* **68**, 37–47 (2009).
42. Tada, S. *et al.* BAFF Controls Neural Cell Survival through BAFF Receptor. *PLoS One* **8** (2013).

Acknowledgements

The authors thank Kyoko Kubota, Kaori Nakano and Shuji Kohri for their secretarial assistance and Kaori Sakakibara for her technical assistance. This study was supported in part by a Health and Labour Sciences Research Grant on Rare and Intractable Diseases (Validation of Evidence-based Diagnosis and Guidelines, and Impact on QOL in Patients with Neuroimmunological Diseases) from the Ministry of Health, Labour and Welfare of Japan and by AMED (Japan Agency for Medical Research and Development).

Author Contributions

S.T., T.O., Y.S., M.K., Y.S., Y.N. and H.M. conceived and designed the study. S.T., T.O., M.S., H.S.-A., K.Y., E.S., C.C., A.N., T.S., T.K., K.T. and S.M. performed the experiments and analyzed the data. S.T., T.O. and E.S. drafted a significant portion of the manuscript. All authors read and approved the final manuscript.

Additional Information

Supplementary information accompanies this paper at <https://doi.org/10.1038/s41598-019-41771-4>.

Competing Interests: The authors declare no competing interests.

Publisher's note: Springer Nature remains neutral with regard to jurisdictional claims in published maps and institutional affiliations.



Open Access This article is licensed under a Creative Commons Attribution 4.0 International License, which permits use, sharing, adaptation, distribution and reproduction in any medium or format, as long as you give appropriate credit to the original author(s) and the source, provide a link to the Creative Commons license, and indicate if changes were made. The images or other third party material in this article are included in the article's Creative Commons license, unless indicated otherwise in a credit line to the material. If material is not included in the article's Creative Commons license and your intended use is not permitted by statutory regulation or exceeds the permitted use, you will need to obtain permission directly from the copyright holder. To view a copy of this license, visit <http://creativecommons.org/licenses/by/4.0/>.

© The Author(s) 2019